

# **Porphyrin Tessellation by Design: Metal-Mediated Self-Assembly of Large Arrays and Tapes\*\***

Charles Michael Drain,\* Fotis Nifiatis,  
Alexander Vasenko, and James D. Batteas

In light of the tremendous versatility of porphyrins and metalloporphyrins in mediating electron and energy transfer, their utility as redox catalysts, and their dynamic photo-physical properties, there have been considerable efforts made in the design and synthesis of oligoporphyrins. These covalent compounds yield information on the mechanisms of electron and energy transfer, and demonstrate the possibility to use these chromophores in photonic devices.<sup>[1]</sup> In the synthesis of discrete ordered arrays of covalently linked porphyrins, there now seems to be a practical limit of about ten macrocycles.<sup>[2]</sup> To create ever larger arrays in reasonable yields, a supramolecular approach has been employed to design a variety of discrete porphyrin arrays;<sup>[3–6]</sup> self-assembly makes use of molecular recognition through hydrogen bonds,<sup>[3]</sup> coordination of transition metal ions,<sup>[4]</sup> electrostatic interactions,<sup>[5]</sup> and self-coordination of metallo derivatives.<sup>[6]</sup> Notably, the largest designed discrete assemblies containing six or more components have been squares made up of four porphyrins assembled by four transition metal ions,<sup>[4]</sup> and a rosette containing six porphyrins assembled by hydrogen bonding.<sup>[3b]</sup>

Herein we push the methodology into the next level of complexity and present the design of a discrete supramolecular array of nine porphyrins (Figure 1). Self-assembly is accomplished by coordination of exocyclic pyridyl groups on three different porphyrin derivatives to 12 palladium(II) dichloride units: Four different types of molecules self-assemble to a 21-membered, array that is 25 nm<sup>2</sup> large.<sup>[7]</sup>

These types of systems are expected to further our understanding of photonic communication between chromophores mediated by noncovalent interactions, serve as a guide for the formation of molecular channels or receptors, and be a foundation for the development of molecular photonic materials such for use in nonlinear optics.<sup>[1, 2]</sup> The well-characterized photophysical behavior of these macrocycles provides a tool for the examination of the kinetics, mecha-

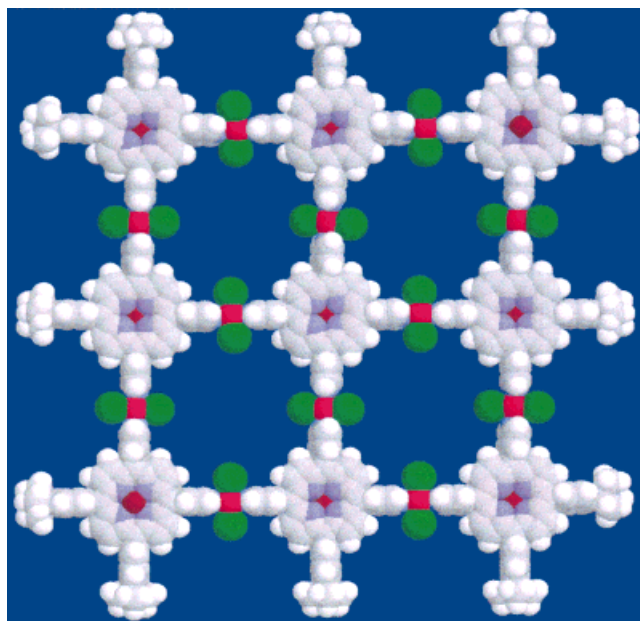


Figure 1. Space-filling model of the tessellated porphyrin **6b**.

nism, and thermodynamics of self-assembly. The formation and characterization of porphyrin squares, whose self-assembly is mediated by one or two different transition metals, have been well documented.<sup>[4]</sup>

We designed the nonameric arrays **5** and **6** by appropriate choice of *trans* coordination by the relatively labile square-planar bis(benzonitrile)palladium(II) dichloride (**4**), the correct stoichiometries of the components, and the correct substitution patterns of three different porphyrins: one central X-shaped unit (porphyrin **1**), four T-shaped units on the sides (porphyrin **2**), and four L-shaped units in the corners (porphyrin **3**; Scheme 1). The “molecular information” inherent in the individual molecules and the stoichiometry (12Pd, 1“X”, 4“L”, and 4“T”) favors the formation of the desired arrays, but the reversibility of pyridyl–palladium bond formation is also crucial for reaching what appears to be the thermodynamic product. Thus, the desired arrays are formed in approximately 90 % yield at room temperature in less than 30 minutes when **4** is added to the correct mixture of porphyrins (total concentration < 10 μM) in chloroform, mineral oil, or toluene. At concentrations of about 20 μM the yield is reduced to less than 70 %. One key feature of this system is that there are three different porphyrins, so any combination of free base and metallo compounds may be used to make the supramolecular arrays. This results in arrays with metallo derivatives in predictable positions. In the present study only the all-free base or all-zinc complexes are presented to avoid the kinetic and spectroscopic complications that arise from axial coordination by the pyridyl groups to other metalloporphyrins (homocoordination).

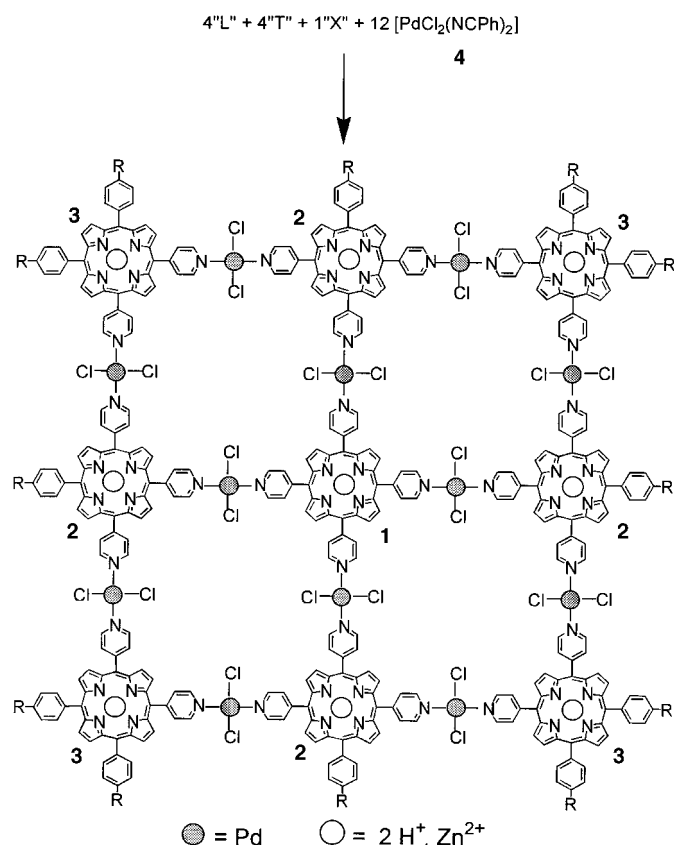
Porphyrin tapes (Scheme 2) are made in a manner similar to that of the nonamers. For example, addition of two porphyrins **7b** (“O”) to two “T”-shaped porphyrins **8b** and two equivalents of **4** results in the palladium-based tape **9b** as a mixture of the dimer, the trimer, and the tetramer in a ratio of about 3:8:2. For tape **10a**, which is made by mixing porphyrins

[\*] Prof. Dr. C. M. Drain, F. Nifiatis, A. Vasenko  
Department of Chemistry at Hunter College  
The City University of New York  
New York, NY 10021 (USA)  
Fax: (+1) 212-772-5332  
E-mail: cdrain@shiva.hunter.cuny.edu

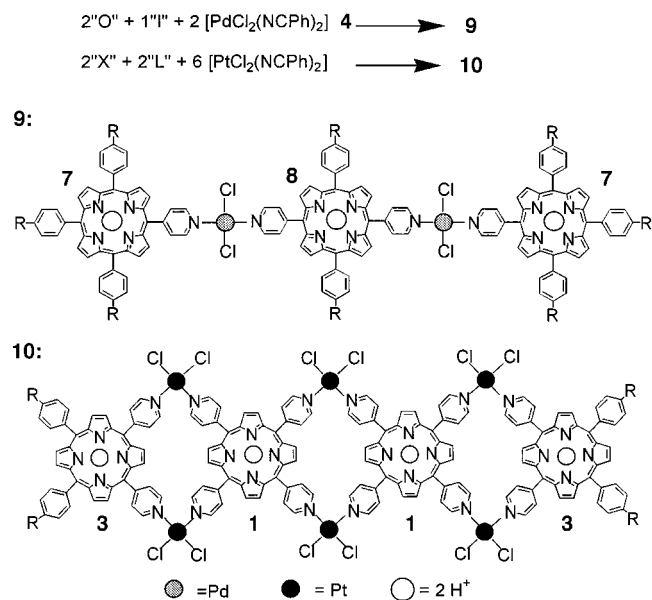
Prof. Dr. J. D. Batteas  
Department of Chemistry at the College of Staten Island  
The City University of New York (USA)

[\*\*] Financial support from RCMI from the National Institutes of Health (RR-03037), New York State GRI grants to Hunter College, a Hunter College Presidential Scholar Fellowship to A.V., the NSF (Career CHE-9732950), and a CUNY Collaborative Research Grant to C.M.D. are gratefully acknowledged. We thank Vinita Tiwari and Suhel Ahmed for help in preparing some of the porphyrins.

Supporting information for this article is available on the WWW under <http://www.wiley-vch.de/home/angewandte/> or from the author.



Scheme 1. Self-assembled planar nonameric arrays of porphyrins. Porphyrins: "T": **2a**, R = methyl; **2b**, R = *tert*-butyl; "L": **3a**, R = methyl; **3b**, R = *tert*-butyl; "X": **1**. Arrays: **5a**, R = methyl,  $\circ = 2\text{H}^+$ ; **5b**, R = *tert*-butyl;  $\circ = 2\text{H}^+$ ; **6a**, R = methyl,  $\circ = \text{Zn}^{2+}$ ; **6b**, R = *tert*-butyl,  $\circ = \text{Zn}^{2+}$ .



Scheme 2. Self-assembled tapes of porphyrins. Porphyrins: "L": **3a**, R = methyl; **3b**, R = *tert*-butyl; "O": **7a**, R = methyl; **7b**, R = *tert*-butyl; "I": **8a**, R = methyl; **8b**, R = *tert*-butyl. Tapes: **9a**, R = methyl,  $\circ = 2\text{H}^+$ ; **9b**, R = *tert*-butyl,  $\circ = 2\text{H}^+$ ; **10a**, R = methyl,  $\circ = \text{Zn}^{2+}$ ; **10b**, R = *tert*-butyl,  $\circ = \text{Zn}^{2+}$ .

**1** and **3** (2 "X" and 2 "L") for 4–5 days at 40 °C, a mixture of the trimer, the tetramer, and the pentamer in a ratio of about 2:4:1 is obtained, as determined by electrospray (ES) mass

spectrometry. The asymmetric distribution of the subunits probably arises for reasons of entropy and solubility.

Titration of **4** into a solution of the porphyrins in toluene, mineral oil, or chloroform results in clear isosbestic points for the Q and B (Soret) bands in the UV/Vis spectra of the porphyrins, indicating the formation of only one species in solution.<sup>[8]</sup> The substantial broadening, concomitant decrease in intensity, and red shift of the Soret band is typical for electronically coupled porphyrins. It is observed to a lesser extent for the Pd-mediated dimer and tetramer arrays and other squares.<sup>[4]</sup> There is a consistent red shift of about 2 nm (and broadening) per porphyrin in going from the linear Pt-linked dimer to tetramer of **10a** and **10b**. This is also observed for the Pd-linked tapes **9a** and **9b**. This and previous UV/Vis data<sup>[4a]</sup> suggest that the number of porphyrins in the array and their relative geometry are of great importance.

The fluorescence emission of a stoichiometric mixture of porphyrins is quenched to greater than 90 % as **4** is titrated into the solution to form the tessellated nonamer **5b**. This is confirmed by the measurements of the excited state lifetime; the average lifetime for a mixture of porphyrins in toluene at room temperature is 12 ns, and that of the array is less than 1 ns.<sup>[9]</sup> There is a quadratic decrease in the intensity of the fluorescence emission of tetrapyrrolylporphyrin (**1**) with each successive binding of a palladium complex  $[\text{Pd}_2\text{Cl}_4(\text{Ph}_3\text{P})_2]$ , which is capable of binding only one pyridyl moiety (confirmed by the fluorescence lifetime studies) and arises due to the heavy-atom effect. From the latter data, one would expect that the nonamer fluorescence should be quenched by about 57 % due to the heavy-atom effect. The substantial additional quenching for the arrays is likely due to energy transfer from one porphyrin moiety to another, and to some  $\pi$  stacking of the nonamers.<sup>[9]</sup>

The  $^1\text{H}$  NMR titrations exhibit similar trends as those observed for other porphyrin squares,<sup>[4]</sup> namely, there is a highly characteristic shift in the pyridyl protons upon coordination of a metal ion. In the starting stoichiometric mixture of the porphyrins (1 "X", 4 "T", and 4 "L") there are four sets of protons  $\alpha$  to the pyridyl nitrogen atom; each signal should be a doublet, but a complex multiplet at  $\delta = 9.05$  is observed in the  $^1\text{H}$  NMR spectrum. As **4** is titrated into a 10  $\mu\text{M}$  mixture of **2b**, **3b**, and **4**, the peaks at  $\delta = 9.05$  decrease in intensity as new resonances at  $\delta = 9.45$  grow. Significantly, the signals for the *tert*-butyl protons shift (from one peak at  $\delta = 1.621$  to two peaks at  $\delta = 1.627$  and  $1.634$  with the expected 2:1 ratio) and broaden slightly, and indicate a greater than 70 % yield for **5b**. Although these new resonances are broader, consistent with the large increase in molecular size and slower tumbling, the line width indicates that the material in solution is of the size expected for **5b**. Similar to previous studies,<sup>[4a]</sup> the zinc porphyrin array **6b** can be titrated with 4.5 equivalents of 4,4'-bipyridine (bpy) to form a sandwich of nine bpy molecules between two nonamer zinc–porphyrin arrays, that is, 18 porphyrins in one system. This is clearly indicated by the new resonances for the  $\alpha$  protons on bpy at  $\delta = 2.2$  and  $5.2$  with a broadening of about 80 %, which again is consistent with the formation of a much larger species and not a collection of polymeric materials.

Light-scattering results suggest that clusters with a radius of 5–7 nm are present in solution. Depending on solution conditions, deposition of nonameric arrays on polished glass substrates results in the formation of nanoparticle clusters. Characterization of the three-dimensional arrangement of these clusters by atomic force microscopy (AFM) suggests that the nonameric arrays deposit as columnar structures on the glass surface, potentially as nanocrystals. The clusters range in height from 1.3 to 39 nm with over 75% between 4.5–6.5 nm, which is consistent with the light-scattering data. Widths of 5 nm for single nonameric arrays on the surface were not observed. However, as the images of the clusters so closely match that of the expected AFM tip profile, the nonamers likely stack as columns on the surface with widths less than that of the nominal radius of curvature of the AFM probe tip (ca. 20 nm). Therefore, such sharp, clear images of the tip structure (Figure 2) strongly suggest the nonamers deposit as stacks on the order of  $5 \times 5 \times 5 \text{ nm}^3$ . These

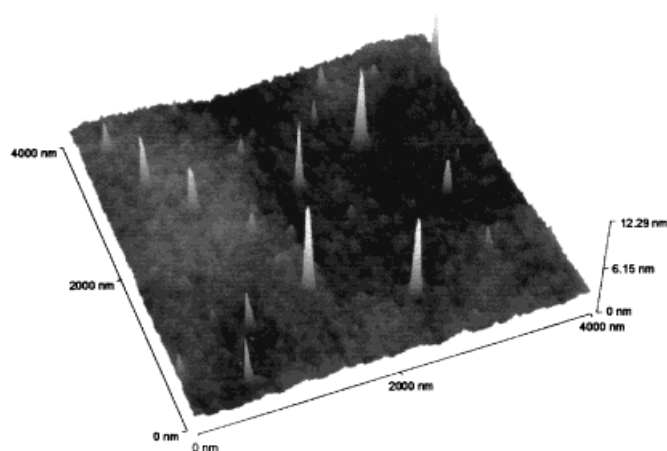


Figure 2. Typical atomic force microscope image of **5b** on a glass surface showing the sharp AFM probe tip structure produced from scanning the columnar stacks of nonameric arrays.

arrangements are induced by a significant intermolecular  $\pi$ -stacking energy per porphyrin face (ca. 5 kcal mol<sup>-1</sup>) depending on solvent and concentration. These nanocrystalline materials are expected to have interesting photo- and electrochemical properties,<sup>[1, 7]</sup> and are currently under investigation.

Other evidence for the formation of the arrays and tapes comes from a variety of methods: dynamic light scattering and size-exclusion chromatography of **5a**, **5b**, **10b**, and **10b**; ES-MS of **10a** and **10b**; and vapor phase osmometry on **5a** and **5b**. Electrospray mass spectra of the four nonameric arrays (in CHCl<sub>3</sub> with 0.3% trifluoroacetic acid or acetic acid) shows the expected signals for molecular ions with charges of 3+ and 4+, consistent with the arrays.<sup>[8]</sup> The highly characteristic envelope due to the various isotopes (especially of Cl and Pd) greatly assist in the identification of the tri- and tetra-protonated nonamer. Peaks consistent with the loss of three and four chloride ions are also observed.<sup>[8]</sup>

The data taken together indicate formation of nonamer arrays that are about 25 nm<sup>2</sup> large, objects that are between discrete chemical species and polymeric materials. This work demonstrates that it is possible to design and self-assemble large, complex arrays of ridged dye molecules such as

porphyrins by choosing the appropriate geometry of the building blocks and metal ions. The properties of these arrays and materials may be readily fine-tuned by the choice of metal ion linker, the metalloporphyrins used, and further substituents on the macrocycle (such as bromo, nitro, and amino groups) at one or more  $\beta$ -pyrrole positions.

### Experimental Section

Porphyrins **1**, **2a**, **3a**, **7a**, and **8a** are prepared by either the Adler<sup>[10a]</sup> or high-temperature methods<sup>[10b]</sup> from a mixture of 4-methylbenzaldehyde, pyridine-4-carbaldehyde, and pyrrole (2:2:4). The six possible compounds were separated on two flash chromatography columns with hexane/toluene/chloroform gradients. Porphyrins **2b**, **3b**, **7b**, and **8b** are made similarly. Although these are new derivatives, the parent pyridyl compounds have been described in the literature. All starting porphyrins gave satisfactory UV/Vis and <sup>1</sup>H NMR spectra, as did all the arrays and tapes. Satisfactory fast atom bombardment (FAB) mass spectra for the starting porphyrins and ES mass spectra for the arrays and tape were also obtained.

Preparation of arrays and tapes (for example, **5b**): To a solution of **1** (0.222  $\mu\text{M}$ ), **2b** (0.888  $\mu\text{M}$ ), and **3b** (0.888  $\mu\text{M}$ ; 1:4:4, 2  $\mu\text{M}$  in porphyrins) is added **4** in four aliquots at intervals of at least five minute to reach a concentration of 2.66  $\mu\text{M}$ . Typically this is done in a 3-mL cuvette, and the reaction is monitored by UV/Vis spectroscopy (see Figure 1 of the Supporting Information). The arrays with the zinc complex are formed in a similar procedure. The nonameric array is more soluble when the methyl group on the phenyl rings is replaced by *tert*-butyl (< 1  $\mu\text{M}$  concentrations of **1a**, **2a**, and **3a** are used to form **5a** and **6a**). When a Pd complex with only one binding site coordinates to a monopyridylporphyrin there is a red shift of about 1 nm and a slight broadening of the Soret band; when **1a** or **1b** coordinate four of these Pd complexes, there is a net red shift of about 4 nm and the broadening is less than 10%. When the solvent is evaporated very small amounts of **5a** and **5b** can be resolubilized, which is most likely due to  $\pi$ -stacking interactions. Thus, the arrays are stored in solution in the dark under an inert atmosphere, where they are stable for months. Tapes **9a** and **9b** are formed by similar procedures (see above), but formation of tapes **10a** and **10b** require vigorous stirring at about 40 °C for 5–6 days under nitrogen in the dark.

AFM data were obtained with a Topometrix Explorer stand-alone microscope in an environmental chamber under dry air with a relative humidity of less than 2%. Data were collected in the attractive noncontact mode to avoid altering the surface features. Imaging in the constant-force DC contact mode was observed to damage the nanoparticles. The glass slides were cleaned, dipped into a 0.5  $\mu\text{M}$  solution of **5a** for 3 h, and dried under vacuum. Control experiments with individual porphyrins, mixtures of porphyrins, and the Pd starting material yield no discernible structures. Many different samples and tips yield the same results. Additionally, these readily prepared structures provide a remarkably consistent way to obtain high-quality probe tip images.

Received: November 25, 1997

Revised version: May 22, 1998 [Z11194IE]

German version: *Angew. Chem.* **1998**, *110*, 2478–2481

**Keywords:** atomic force microscopy • coordination chemistry • nanostructures • porphyrinoids • supramolecular chemistry

- [1] a) J.-M. Lehn, *Supramolecular Chemistry: Concepts and Perspectives*, VHC, Weinheim, **1995**; b) J. S. Lindsey, *New J. Chem.* **1991**, *15*, 153–180.
- [2] a) S. Anderson, H. L. Andersen, J. K. M. Sanders, *J. Chem. Soc. Perkin Trans. 1* **1995**, 2247–2254; b) D. L. Officer, A. K. Burrell, D. C. W. Reid, *Chem. Commun.* **1996**, 1657–1658; c) D. Fenyo, B. T. Chait, T. E. Johnson, J. S. Lindsey, *J. Porphyrins Phthalocyanines* **1997**, *1*, 93–99.
- [3] a) C. M. Drain, R. Fischer, E. Nolen, J.-M. Lehn, *J. Chem. Soc. Chem. Commun.* **1993**, 243–245; b) C. M. Drain, K. C. Russell, J.-M. Lehn, *Chem. Commun.* **1996**, 337–338.

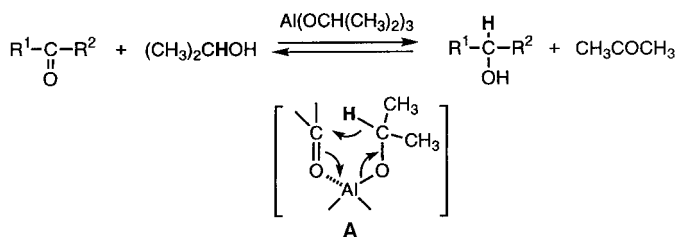
- [4] a) C. M. Drain, J.-M. Lehn, *J. Chem. Soc. Chem. Commun.* **1994**, 2313–2315; b) H. Yuan, L. Thomas, L. K. Woo, *Inorg. Chem.* **1996**, *35*, 2808–2817; c) P. J. Stang, J. Fan, B. Olenyuk, *Chem. Commun.* **1997**, 1453–1454; d) R. V. Slone, J. T. Hupp, *Inorg. Chem.* **1997**, *36*, 5422–5437.
- [5] a) C. M. Drain, D. Mauzerall, *Biophys. J.* **1992**, *63*, 1556–1563; b) K. Araki, M. J. Wagner, M. S. Wrighton, *Langmuir* **1996**, 5393–5398.
- [6] K. Funatsu, A. Kimura, T. Imamura, Y. Sasaki, *Chem. Lett.* **1995**, 765–766.
- [7] While coordination polymers have been known for many decades, the formation of discrete ordered coordination arrays is enjoying a renaissance: a) J.-M. Lehn, *Angew. Chem.* **1990**, *102*, 1347–1362; *Angew. Chem. Int. Ed. Engl.* **1990**, *29*, 1304–1319; b) M. Fujita, Y. J. Kwon, S. Washizu, K. Ogura, *J. Am. Chem. Soc.* **1994**, *116*, 1151–1152; c) R. V. Slone, J. T. Hupp, C. L. Stern, T. E. Albrecht-Schmitt, *Inorg. Chem.* **1996**, *35*, 4096–4097; d) B. Linton, A. D. Hamilton, *Chem. Rev.* **1997**, *97*, 1669–1680; e) P. J. Stang, B. Olenyuk, *Acc. Chem. Res.* **1997**, *30*, 507–518.
- [8] a) The UV/Vis spectra (see Figure 1 of the Supporting Information) were measured with a 0.5  $\mu\text{M}$  solution in toluene (formation of nonamer **5b** from the porphyrin mixture **1** + **2b** + **3b**); Soret bands (half-width) in nm (porphyrin mixture  $\rightarrow$  **5b**): 418.9 (15.3)–408.4 (23.2), 425.9 (18.2), 439.6 (20.4). b) The ES mass spectrum (HP-1100 LC/MS, direct injection at 0.1 mL min<sup>-1</sup>, N<sub>2</sub> carrier gas at 1 mL min<sup>-1</sup>, ionization potential 150 kV, positive-ion mode) of **5a** in CHCl<sub>3</sub> with 0.3 % acetic acid (see Figure 3 of the Supporting Information) shows the tri- and tetra-protonated nonamer at  $m/z$  = 2619 and 1965, respectively. Additionally, it shows the loss of three and four chloride ions at  $m/z$  = 2583 and 1928, respectively. Vapor-phase osmometry studies used toluene as solvent and were standardized with polystyrene of a known average molecular weight. c) <sup>1</sup>H NMR (300 MHz, CDCl<sub>3</sub>; see Figure 4 of the Supporting Information) for nonamer **5b** formed from **1** + **2b** + **3b**:  $\alpha$ -pyridyl ( $\delta$  = 9.051  $\rightarrow$  9.454),  $\beta$ -pyridyl ( $\delta$  = 8.13  $\rightarrow$  8.32), *tert*-butyl ( $\delta$  = 1.621  $\rightarrow$  1.627 and 1.634), pyrrole NH ( $\delta$  = -2.816, -2.866, -2.906  $\rightarrow$  -2.786, -2.811, -2.840). The width at half-height of the methyl peaks broadens from about 2 Hz to 4.2 Hz.
- [9] Fluorescence quenching (supramolecular array/porphyrin mixture at the same optical density): **5a** (ca. 87 % in toluene, ca. 93 % in CCl<sub>4</sub>), **5b** (>90 % in CHCl<sub>3</sub> or mineral oil), **9a** (14 % in toluene), **10a** (18 % in toluene). The complete photophysical characterization of these systems will be reported elsewhere.
- [10] a) A. D. Adler, F. R. Longo, W. Shergalis, *J. Am. Chem. Soc.* **1964**, *86*, 3145–3148; b) C. M. Drain, X. Gong, *Chem. Commun.* **1997**, 2117–2118.

## Highly Efficient, Catalytic Meerwein–Ponndorf–Verley Reduction with a Novel Bidentate Aluminum Catalyst\*\*

Takashi Ooi, Tomoya Miura, and Keiji Maruoka\*

The Meerwein–Ponndorf–Verley (MPV) reaction, named after the independent originators, involves the chemoselective reduction of carbonyl substrates with aluminum alkoxides, generally Al(O*i*Pr)<sub>3</sub>, as catalyst and *i*PrOH as hydride source.<sup>[1–3]</sup> In the MPV reduction, a reversible hydride transfer from the alcoholate to a carbonyl acceptor via a six-

membered transition state **[A]** is initiated by the activation of the carbonyl group by coordination to the Lewis acidic aluminum center (Scheme 1).<sup>[4]</sup> Acetone is formed as a



Scheme 1. MPV reduction of carbonyl compounds with Al(O*i*Pr)<sub>3</sub> in *i*PrOH, which proceeds via transition state **A**.

volatile side product, which is easily removed during the reaction. Advantages of the MPV reduction include chemoselectivity, mild reaction conditions, operational simplicity, safe handling, and ready adaptation both in the laboratory and on a large scale.<sup>[5]</sup>

Nonetheless, there are several practical problems with the MPV reduction such as the need for an excess of alcohol as hydride source, low reaction rate, formation of condensation products, and need for higher reaction temperatures so that the concurrent removal of acetone shifts the equilibrium towards the formation of alcohol. The most important side reactions are the aldol condensation and the Tishchenko reaction; the latter leads to the formation of carboxylic esters, especially in the case of the more reactive aldehydes.<sup>[6]</sup> Accordingly, various modifications of the MPV reduction have been developed in order to overcome these disadvantages. The more recent improvements are the use of catalytically active lanthanide alkoxides,<sup>[7]</sup> microwave irradiation,<sup>[8]</sup> and the addition of CF<sub>3</sub>CO<sub>2</sub>H to Al(O*i*Pr)<sub>3</sub> to accelerate the reduction.<sup>[9]</sup> Herein we report the highly accelerated MPV reduction of carbonyl substrates with a bidentate aluminum catalyst. The realization of this modern MPV reduction is crucially dependent on the effective use of our recently developed bidentate Lewis acid chemistry.<sup>[10]</sup>

The typical MPV reduction of carbonyl substrates proceeds quite reluctantly. For example, reduction of benzaldehyde in CH<sub>2</sub>Cl<sub>2</sub> with Al(O*i*Pr)<sub>3</sub> (1 equiv) at room temperature for 1 h gave rise to benzyl alcohol in 34 % yield.<sup>[11]</sup> When the reaction was carried out in CH<sub>2</sub>Cl<sub>2</sub> with *i*PrOH (1 equiv) and a catalytic amount of Al(O*i*Pr)<sub>3</sub> (10 mol %) at room temperature for 2 h, benzyl alcohol was obtained in only 10 % yield (Table 1). Under similar reduction conditions, ketone substrates (e.g., 4-phenylcyclohexanone and 2-undecanone) were totally unreactive, and most of the starting material was recovered. In marked contrast, however, use of the bidentate aluminum catalyst **1** in the reduction of benzaldehyde produced the benzyl alcohol at room temperature instantaneously and almost quantitatively (Scheme 2). Catalyst **1** is generated in situ from 2,7-dimethyl-1,8-biphenylenediol, Me<sub>3</sub>Al (2 equiv), and *i*PrOH (4 equiv). Moreover, even with 5 mol % of **1** the reduction proceeds quite smoothly at room temperature to furnish benzyl alcohol in 81 % yield after 1 h. This remarkable efficiency can be ascribed to the double

[\*] Prof. K. Maruoka, Dr. T. Ooi, T. Miura  
Department of Chemistry, Graduate School of Science  
Hokkaido University  
Sapporo, 060–0810 (Japan)  
Fax: (+81) 11-746-2557  
E-mail: maruoka@sci.hokudai.ac.jp

[\*\*] This work was partially supported by a Grant-in-Aid for Scientific Research from the Ministry of Education, Science, Sports and Culture, Japan.